Impact of bacterial activity on turnover of insoluble hydrophobic substrates (phenanthrene and pyrene)—Model simulations for prediction of bioremediation success

Rein, Arno; Adam, Iris K.U.; Miltner, Anja; Brumme, Katja; Kästner, Matthias; Trapp, Stefan

Published in:
Journal of Hazardous Materials

Link to article, DOI:
10.1016/j.jhazmat.2015.12.005

Publication date:
2016

Document Version
Peer reviewed version

Incomplete, not-final pre-print version. To get the final version see here:

http://www.sciencedirect.com/science/article/pii/S030438941530265X

Model simulations and impact of bacterial activity on turnover and bioremediation of insoluble hydrophobic substrates (phenanthrene and pyrene)

Arno Rein [1,x,a], Iris K. U. Adam [2,x], Anja Miltner [2], Katja Brumme [2], Matthias Kästner [2,+,*], Stefan Trapp [1,+]

[1)] Department of Environmental Engineering, Technical University of Denmark, Miljøvej bd. 113, DK-2800 Kgs. Lyngby, Denmark.

[2)] UFZ - Helmholtz-Centre for Environmental Research, Department of Environmental Biotechnology, Permoserstr. 15, 04318 Leipzig, Germany.

*****) Corresponding author; phone +49341235-1235; fax: +49341235-451235; e-mail: matthias.kaestner@ufz.de

[x]) both authors contributed equally to this work

[+]) both authors contributed equally to this paper and to the organization of the project

[a)] present address: Chair of Hydrogeology, Technical University of Munich, Arcisstr. 21, 80333 Munich, Germany

Abstract

Many attempts for bioremediation of polycyclic aromatic hydrocarbon (PAH) contaminated sites failed in the past, but the reasons for this failure are not well understood. Here we apply and improve a model for integrated assessment of mass transfer, biodegradation and residual concentrations for predicting the success of remediation actions. First, we provide growth parameters for *Mycobacterium rutilum* and *M. pallens* growing on phenanthrene (PHE) or pyrene (PYR) degraded the PAH completely at all investigated concentrations. Maximum metabolic rates V_{max} and growth rates μ were similar for the substrates PHE and PYR and for both strains. The investigated *Mycobacterium* species were not superior in PHE degradation to strains investigated earlier with this method. Real-world degradation scenario simulations including diffusive flux to the microbial cells indicate: that i) bioaugmentation only has a small, short-lived effect; ii) Increasing sorption shifts the remaining PAH to the adsorbed/sequestered PAH pool; iii) mobilizing by solvents or surfactants resulted in a significant decrease of the sequestered PAH, and iv) co-metabolization e.g. by compost addition can contribute significantly to the reduction of PAH, because active biomass is maintained at a high level by the compost. The model therefore is a valuable contribution to the assessment of potential remediation action at PAH-polluted sites.

Keywords: PAH-degradation, mycobacteria, growth, kinetics, modelling, bioremediation-options.

1. Introduction

Polycyclic aromatic hydrocarbons (PAH) are hydrophobic compounds with two or more condensed benzene rings in their molecular structure [1]. They exhibit high toxicity and cancerogeneity [2]. PAH are metabolised by several bacteria, fungi, algae and also by cytochrome P-450 monooxygenases of higher eukaryotic cells [3], but undergo no or slow decomposition in the environment [4]. Full mineralisation with productive growth is only known for bacteria [5]. However, reports about full mineralisation of PAH with > 5 rings are relatively rare [6].

Varying concentrations of PAH occur in coals, crude oils and oil-based products. They are formed during pyrolysis and incomplete combustion of biological material and organic compounds and thus one main source of the anthropogenic formation and emission of PAH is the combustion of fossil fuels in vehicles and for power generation [7]. Due to their properties, PAH are released during combustion adsorbed to dust and soot particles, and are then more or less globally distributed in the environment [8]. PAH also frequently occur in urban soil environments due to the process of coal gasification in the 19^{th} century [9] leading to the formation of waste tar oils often dumped in open pits at the manufactured gas plant sites. Later with increasing urbanisation the tar oil ponds were solidified with waste coke materials and coal powders that could not be burned in the plants at that time. These widespread contaminations entered focus in the late 1980s and gas works sites or sites where tar oil products were spilled were identified to need technical soil remediation. Many attempts for bioremediation failed without real understanding of the reasons, most probably because PAH tend to sorb strongly to coal and coke particles or to so-called non-aqueous phase liquids (NAPL) soil [3]. The biodegradation of the hardly water-soluble PAH is typically limited by the diffusive flux to the microbes. Aging or sequestration was considered to lower the bioavailability of these compounds, since sorption to soil gets stronger (K_d increases) with time and degradation half-times increase with time, resulting in a fraction of persistent compounds [10, 11].

Recently a modelling approach for integrated mass transfer, biodegradation (parameter determination: v_{max}, K_M and yield) and residual concentration assessment was developed and applied for the turnover of non-water soluble substrates like PAH under mass transfer limitations [5, 12]. The model equations imply that below a certain substrate concentration, or more exactly below a certain substrate flux to the microorganisms, bacterial growth ceases and bacterial populations start to decline which in turn leads to non-degraded residues. For the prospective assessment of the turnover of PAH there is a research gap since only very limited kinetic data for different groups of PAH degrader bacteria are available. In particular for mycobacteria the knowledge is limited [13] due to the complex cell cycle with formation of cell clusters and aggregates with PAH.

The goal of the present work is to determine and compare growth and affinity parameters for well described phenanthrene (PHE) and pyrene (PYR) degrading mycobacteria on both substrates. In addition, the unified modelling approach for sorption and degradation [5, 12] was improved and applied to prospectively describe the dynamics of the PAH compound turnover for various treatment options for soil at contaminated sites. Simulated treatment options include bioaugmentation measures, the addition of adsorbing amendments for reducing pollutant mobility, the addition of solvents or chelators for increasing pollutant dissolution, as well as measures for stimulating co-metabolism (addition of co-substrates such as compost).

2. Materials and Methods

2.1. Strains and culture conditions.

For the comparative assessment of degradation kinetics, the well described *Mycobacterium rutilum* (PHE and PYR degraders) and *Mycobacterium pallens* (PYR degrader) were chosen as model microorganisms [14] based on their multiple PAH degradation (PHE and PYR),

96 growth kinetics in liquid cultures and their origin from different environmental samples (Table
97 1).

98 The strains were pre-cultivated on mineral medium (MM) with vitamins (Brunner, DSMZ no.
99 462) consisting of Na_2HPO_4 2.44·gL^{-1}, KH_2PO_4 1.52·gL^{-1}, $(NH_4)_2SO_4$ 0.5·gL^{-1}, $MgSO_4x7H_2O$
100 0.2·gL^{-1}, $CaCl_2x2H_2O$ 0.05·gL^{-1}, trace element solution SL-4 10·mLL^{-1} (containing per L^{-1}:
101 EDTA 0.5·g, $FeSO_4x7H_2O$ 0.2·g and trace element solution SL-6 100·mLL^{-1} [containing per L^{-1}
102 $ZnSO_4x7H_2O$ 0.1·g, $MnCl_2x4H_2O$ 0.03·g, H_3BO_3 0.3·g, $CoCl_2x6H_2O$ 0.2·g, $CuCl_2x2H_2O$
103 0.01·g, $NiCl_2x6H_2O$ 0.02·g, $Na_2MoO_4x2H_2O$ 0.03·g]) and 2.5·mLL^{-1} vitamin solution consisting
104 of p-aminobenzoate 10·mgL^{-1}, biotin 2·mgL^{-1}, nicotinic acid 20·mgL^{-1}, thiamine-$HClx2H_2O$
105 10·mgL^{-1}, Ca-pantothenate 5·mgL^{-1}, pyridoxamine 50·mgL^{-1}, vitamin B_{12} 20·mgL^{-1} [15]. PHE
106 (98% purity, Sigma-Aldrich, Saint Louis, USA) or PYR (>96% purity, Merck Schuchardt,
107 Hohenbrunn, Germany) was provided as a sole source of carbon and energy.

108 *2.2. Experimental set-up.*

109 To overcome the inhomogeneities of PAH cultures with total concentrations above water
110 solubility, a 'mini-culture approach' [5] for enabling initially non-limited growth on PAH was
111 developed. Briefly, a set-up of destructively sampled small vials (10·mL with finally 2·mL
112 culture) containing 1800·µL of MM was applied in which the initially introduced PHE or PYR
113 solution in acetone was evaporated and the remaining PAH microcrystals were allowed to
114 equilibrate with the MM overnight. The acetone was then allowed to fully evaporate while
115 shaking the vials for covering the bottom surface with a PHE or PYR microcrystal layer
116 corresponding to nominal medium concentrations of 10, 25, 50, 100, 200 and 400·mgL^{-1}
117 (only 100·mgL^{-1} for pre-cultures) prior to adding the MM. The vessels were inoculated to an
118 initial optical density of 0.01 at 560 nm by adding 200 µl of a pre-culture under similar
119 medium conditions at the late exponential phase and incubated at 30°C at 135 rpm. Finally,
120 the vessels were closed with teflon coated butyl rubber septa for cultivation. Each vessel was
121 destructively sampled and analysed at the respective sampling time. The experiment was

performed in six replicates for each concentration and time for providing two triplicate sets for separate quantification of biomass and PHE or PYR. They were harvested after 0, 4, 8, 12, 24, 36, 48, and 96·h of incubation for initial 10, 25 and 50·mgL^{-1} PHE or PYR concentrations and after 0, 6, 12, 24, 48, 72, 96, 192 and 288·h for initial 100, 200 and 400·mgL^{-1} PHE or PYR conc. for both strains (*M. rutilum* and *M. pallens*). The harvested cultures were stored at -20°C until further analysis.

2.3. Protein analysis.

For monitoring the growth of the bacteria, we tried to measure the protein photometrically in 96 well plates (BIO-RAD-Protein-Assay, Bio-Rad Laboratories GmbH, München, Germany) as described previously [5]. The protein measurements for both mycobacteria were highly variable due to the cell cycle of these bacteria and due to clustering with the microcrystals (see Supporting Material SM). The optical density at 560 nm (*OD*) measured after rigorous shaking of the cultures gave more consistent results than the direct measurement of the microbial protein concentration and was used to monitor bacterial growth in the degradation experiments. Microbial protein concentrations C_X were then calculated from *OD* under consideration of the microcrystals of the chemicals (PHE or PYR) in solution using the conversion factor f_{CX} (see SM, Figures SM2 and SM3).

2.4. PAH analysis.

For tracking the PAH consumption the mini cultures were extracted two times with 2 ml of hexane with fluorene as internal standard and analyzed by GC-MS as described previously [5]. Briefly, PYR and PHE were quantified by means of a gas chromatograph equipped with a BPX5 column coupled to a mass spectrometer (5975C, Agilent Technologies). The GC oven temperature was programmed to initial 40°C (2 min hold), then heat to 180°C (2 min hold) at 40°Cmin^{-1}, to 240°C (2 min hold) at 5°Cmin^{-1} and to a final temperature of 300°C (5 min hold) at 15°Cmin^{-1} with a helium flow of 1.5ml min^{-1}. The injector was set to 280°C. The MS was operated in the electron impact ionization mode at 70 eV. The source temperature was set to

230°C, the quadrupole temperature to 150°C. Full scans were acquired in the m/z range 40-500.

2.5. Modelling.

The model is a set of ordinary differential equations (spatial dependencies are not considered) with chemical mass *m* as state variable. It includes dissolution of PAH from microcrystals or NAPLs into water (diffusive flux driven by the chemical activity gradient), microbial biodegradation (*Michaelis-Menten* kinetics) and growth kinetics (*Monod* kinetics) including growth delay, maintenance requirements, death and decay rates as described previously in detail [5]. Briefly, these equations are:

$$\frac{dm_{ph}}{dt} = P \times A_{ph} \times \left(S - C_W\right) \quad (1)$$

$$\frac{dm_M}{dt} = \frac{v_{\max} \times C_W}{K_M + C_W} \times X = v \times X \quad (2)$$

$$\frac{dX}{dt} = \left(\frac{dm_M}{dt} - X \times r \right) \times Y \quad (3)$$

$$\frac{dm_W}{dt} = + \frac{dm_{ph}}{dt} - \frac{dm_M}{dt} \quad (4)$$

where Eq. (1) describes dissolution flux (mass from organic PAH phase m_{ph}), Eq. (2) metabolic flux (m_M is metabolized PAH mass), Eq. (3) microbial growth (microbial mass *X*) and Eq. (4) change of PAH mass m_W in water. *S* is water solubility (mgL^{-1}), concentration *C* is *m*/*V*, with mass *m* (g or mg) and volume *V* (L or m^3). C_W (mgL^{-1}) is freely dissolved concentration, the total PAH concentration in suspension is $C_{Sus} = (m_{ph}+m_W)/V$. The equation system includes degradation (Monod kinetics) parameters v_{max}, K_M, *Y*, *b,* maintenance *r* is given as $r = b/Y$ (parameter names and units see Table 2). Parameters for dissolution kinetics are permeability or mass transfer coefficient *P* (md^{-1}) and surface area of PAH phase

A_{ph} (m^2), which is calculated from m_{ph} and correction factor f_A for deviations from cubic geometry (details see SM).

Lag phases, which occurred in most of the experiments, were considered by determining a time t_{lag} by which microbial degradation is delayed, i.e. metabolic flux dm_M/dt was set to zero for times $t \leq t_{lag}$. Eq. (2) modifies accordingly by multiplying metabolic flux dm_M/dt with f_{tlag} which is either 1 or 0,

$$f_{tlag} = \begin{cases} 0 & if \quad t \leq t_{lag} \\ 1 & if \quad t > t_{lag} \end{cases} \tag{5}$$

and this was realized within MATLAB™ by using a modified Heaviside function [16].

The considered model approach is improved and simplified compared to our previous study [5], as kinetic fitting parameters have been reduced from 7 to 6 (the four Monod parameters, t_{lag} and f_A). Moreover, f_A is the only fitting parameter for dissolution, and t_{lag} only evokes a delay in the onset of degradation. This simplicity is an advantage and further development compared to the approach in Adam et al. [5] where two fitting parameters for dissolution kinetics ($f_{A,0}$ and k_{agg}) were applied and high values of the fitting parameter for the lag phase (factor $f_{inh,corr}$) took influence over the entire duration of the experiment, not only during the time of the lag phase. The parameter t_{lag} is easy to determine (adjusted for the individual experiments), and different f_A can be considered for obtaining model curves at best estimate as well as minimum and maximum estimates for the range of reasonable curve fits. Applying t_{lag} (Eq. 5) needs only one parameter and results in a sudden “step-like” change (zero metabolic flux during the lag phase). As some observations may suggest a gradual onset of PAH degradation, rather than a sudden start, additional model studies were done with f_{tlag} approaching 1 exponentially within t_{lag} (improving only some curve fits slightly; results not shown).

All differential equations were solved numerically, both by an Euler one-step solution scheme realized as Microsoft-Excel™-spreadsheet and by the ODE45-solver (Runge-Kutta-scheme

194 with variable step size) within MATLAB™-R2014b. The correct implementation of the model
195 was quality-controlled by comparing both numerical solutions and by verification against
196 analytical (steady-state) solutions offered by the Best equation. The Best equation balances
197 diffusive flux to the bacterium with metabolic flux in a steady state, thus considering equal
198 and temporally constant dissolution and degradation kinetics (for details see [17]). These
199 conditions were mimicked with the dynamic model (solving Eq. 1 to 5 numerically) by starting
200 with initial conditions at steady-state, where identical results were obtained.

201

202 *2.6. Determination of kinetic parameters.*

203 Bacterial growth and yield parameters were fitted by inverse modeling, i.e. least-square fitting
204 with manual adjustment of parameters, and parameter sensitivity was investigated. Details
205 on the fitting procedure are given in the following and the SM (Section 3). Statistical data on
206 the curve fits (root-mean-square-errors, mean-absolute-errors and coefficients of
207 determination) are provided in Table SM2 for all simulations. The parameters for degradation
208 kinetics (v_{max}, K_M, Y, b), and dissolution kinetics (f_A) were determined iteratively for each
209 bacterial strain until a combination was found that is optimal for all sets of experiments (initial
210 nominal concentrations 10, 25, 50, 100, 200 and 400 mgL^{-1}). Furthermore, lag phases
211 (parameter t_{lag}) were adjusted individually for each experiment. In principle we followed the
212 fitting procedure suggested by Adam et al. [5], i.e. first, the death rate constant b was found
213 from experiments with low initial substrate concentration, then v_{max} and K_M were fitted,
214 followed by the adjustment of Y, with subsequent re-iterations to improve the curve fits.

215

216 **3. Results**

217 The results for *M. rutilum* PHE and PYR degradation with measured versus modeled
218 suspension concentration C_{Sus} and estimated versus modeled microbial protein

concentration $C_{X,est}$, are shown in figures 1 and 2. The input data and the parameters obtained for growth and degradation of the strains are summarized in Table 2. PHE and PYR were degraded virtually completely at all initial concentrations (10, 25, 50, 100, 200, and 400·mgL^{-1}) within t< 4 d for initial $C_{Sus} \leq 100 \cdot mgL^{-1}$ and t=8-12 d for initial $C_{Sus} \geq 100 \cdot mgL^{-1}$ in the fitted curves. Bacterial growth was observed at the first 0.5-2 days and was higher at higher initial substrate concentration. Depletion of substrate led to reduced growth and later decay. The simulations were performed with the same half-saturation constants K_M for all strains (Table 2, 0.1·mgL^{-1}) and succeeded in most cases.

Kinetic parameters for growth of *M. rutilum on* PHE were found as follows: v_{max} = 10 (range 7-12) g·g^{-1}·bact·d^{-1}, K_M = 0.1·mgL^{-1}, b = 0.03 d^{-1}, Y = 0.2 (range 0.16-0.28) g·bact·g^{-1}. Numbers are best estimate values, with ranges (minimum to maximum estimates) in brackets. Lag phases for the experiments ranged from 0.1- 0.3 days (Table SM1).

The yield Y for growth of *M. rutilum* on PYR was relatively similar as for growth on PHE, with a best estimate of 0.22 g·bact·g^{-1}, and the best estimate for v_{max} is 9 g·g^{-1}·bact·d^{-1} (range 7-11). The simulation succeeded with the same values for K_M of 0.1· mgL^{-1} and b of 0.03 d^{-1}. Fitted lag phases (t_{lag}) range from 0-0.8 days (Table SM1). Growth and substrate consumption in these experiments are closely related and decline at the same time (Figures SM2 and SM3).

For *M. pallens* growing on PYR (Figs. SM4 and SM5), the yield (Y = 0.32 g·bact·g^{-1} as best estimate; Table 2) is higher than for *M. rutilum* growing on PYR, whereas v_{max} is similar with 8 g·g^{-1}·bact·d^{-1} as best estimate (range 6-10 g·g^{-1}·bact·d^{-1}). *M. pallens* showed a lower death rate b (0.01 d^{-1}) and the same K_M (Table 2) but a longer lag phase (Table SM1) compared to *M. rutilum* on PYR.

4. Discussion

PHE and PYR were degraded by the tested *Mycobacterium* strains at all initial concentrations accompanied by growth and subsequent decay after substrate consumption. Kinetic data (v_{max}, K_M and Y) were obtained by non-linear fit of a *Monod*-type model. The non-linear fit gave similar maximum metabolic turnover rates for growth of *M. rutilum* and *M. pallens* on PYR. The yields and the decay rates differed slightly. v_{max} for growth on PYR is slightly lower than for growth on PHE, but the yields are higher. The likely ranges overlap and the differences might therefore not be significant. The lag phase for growth on PYR for *M. rutilum* was slightly longer than with PHE as substrate but the difference is insignificant ($P > 0.5$, paired t-test, two-tailed), while the lag phase of *M. pallens* with growth on PYR is clearly longer than that of *M. rutilum* ($P = 0.057$).

Earlier data obtained for growth of three bacterial strains on PHE in the same set-up gave higher results for the maximum metabolism rate v_{max}: Adam et al. [5] determined v_{max} values between 12 and 18 $g \cdot g^{-1} \cdot bact \cdot d^{-1}$ for the strains *Novosphingobium pentaromativorans, Sphingomonas sp.* EPA505 and *Sphingobium yanoikuyae*. The microbial yield was similar with 0.21 $g \cdot g^{-1}$ in the earlier study. Values for the half-saturation constant K_M show no difference ($K_M = 0.1 \cdot mg/L$ in all cases) but this parameter is rather insensitive and other values would hardly alter the fit. The bacterial decay rate constant was slightly lower for the mycobacteria, with $b = 0.01\text{-}0.03\ d^{-1}$ compared to $b = 0.04\text{-}0.05\ d^{-1}$ found for Gram-negative degraders.

The estimates of v_{max} for the *Mycobacterium* species growing on PHE or Pyr carry substantial uncertainty: The measurement of microbial protein concentrations of *Mycobacterium* sp. provided difficulties. Direct measurement of microbial protein gave highly variable and non-plausible values. Optical density was used instead, and the effect of PAH on OD had to be subtracted (SM Section 1). Mycobacteria exhibit a pronounced cell cycle and tend to grow attached to the surface of the PAH crystals [13], and this may be the explanation for the considerable scatter and uncertainty in the estimated microbial protein concentration data.

This attachment may also lead to slower dissolution of the PAH crystals, due to less contact between aqueous phase and crystals.

Wick et al. [13] used solid anthracene as growth substrate for *Mycobacterium* sp. LB501T. They obtained yields Y between 0.158 and 0.196 g·biomass·g^{-1}·substrate·d^{-1}. The decay rate *b* was determined to 0.017 d^{-1} from zero-growth and to 0.048 d^{-1} from nonlinear fit, K_M *was* 0.0428·mgL^{-1} and the maximum metabolic rate v_{max} was 18.4 g·substrate·g^{-1}·biomass·d^{-1}. The estimated v_{max} is higher than the values obtained in our study but was accompanied by lower yields. Maximum growth rates μ_{max} are obtained by v_{max}·×·Y. The μ_{max} for the mycobacteria ranged from 1.98 to 2.56 d^{-1} and were thus lower than those obtained by Adam et al. [5] (2.52-3.78 d^{-1}) and Wick et al. [13] (2.9-3.59 d^{-1}). A relation to water solubility could not be established, the water solubility of anthracene is 0.048·mg/L, of PHE 1.15·mgL^{-1}, and of PYR 0.135·mgL^{-1} [18].

Modeled substrate concentrations yielded predominantly good estimations with coefficients of determination R^2 above 0.95 in most cases. Curve fits for microbial protein concentration C_X were generally less satisfying than those for substrate concentration (Tab. SM2). This can be attributed to uncertainties associated with the determination of C_X from optical density measurements (as discussed above) and the scattered results. The R^2-values obtained show strong variations between individual experiments, predominantly ranging between 0.41 and 0.94. Estimations are often better at higher initial substrate concentration. In some cases C_X decreased during the lag phase, before microbes start to grow (within the first 0.2 to 0.5 days, e.g. Fig. 1a to d). Since the model does not consider specific processes during the lag phase but simply sets growth to zero, deviations to measurements occurred. The lowest R^2 (0.056, Tab. SM2) was obtained for the fit of the *M. rutilum* biomass C_X at the lowest dose of PHE (Fig. 1a), where the fit is impacted by a very high C_X at t = 0.5 d.

4.1. Role of desorption and dissolution in biodegradation of insoluble substrates

296 Sorption processes to solid matter and dissolution from NAPLs are limiting the mass transfer
297 and are causing residual non-degradable concentrations in real contaminated sites [12]. As
298 stated previously [5], the model assumes that transport and bacterial uptake of compounds
299 occurs via the water phase. Even for the mycobacteria no indication was found that transport
300 may also be enabled directly from the organic phase/crystal to the cell surface plus
301 membrane and the transfer and turnover processes can sufficiently be described without
302 considering direct transfer. Considering direct uptake from crystals or NAPLs in the model
303 would not change the kinetics, because in all cases the driver for uptake and metabolism is
304 the chemical activity in solution (maximum activity = water solubility). This is at the same time
305 the activity of the pure solid phase in contact to water [19]. The flux of the substrate to the
306 microbes is the limiting factor. Increasing the dissolution kinetics and the flux to their
307 enzymes by various means, e.g. increase of the surface of mobilization by exudates acting
308 as solvents or biosurfactants or by altering their cell surface properties is therefore a more
309 promising strategy for bacteria than metabolizing solid or NAPL phase substrate directly [5].
310 The effect of these strategies may be larger if the microbes grow in direct contact to the
311 crystals.

312 *4.2 Sorption and mass transfer*.

313 PAH at real contaminated sites are mixed contaminations in a tar oil matrix in most cases
314 and the partitioning equilibrium of single compounds between the tar oil and the water phase
315 are determined by the chemical activity of each compound in the oil matrix expressed by the
316 Raoult´s law; K_d or K_{oc} values of PAH determined in short-term laboratory experiments are
317 not representing the situation in real contaminated soils with or without ongoing degradation.
318 The apparent K_d values in such soils (i.e. the concentration ratio between
319 adsorbed/sequestered and freely dissolved molecules) are not constant, since K_d increases
320 with time due to sequestration or aging (Figures 3a, 3d) [10]. In addition, the apparent K_d
321 increases due to bacterial degradation, which lowers primarily the concentration in dissolved
322 state as long as degradation is ongoing. For the often observed persistence of the

compounds in real environmental systems, increasing half-lives may be due to less substrate present in the dissolved phase. The often postulated irreversible sorption [20] is not required to explain the phenomenon of environmental persistence. After long periods of aging at real contaminated sites, the slow desorption flux of PAH from the sequestered or from the residual tar oil fraction is the only remaining source of compound and limits bacterial growth and metabolism.

4.3. Limitations of growth.

In general, not only the carbon source but also nutrients may limit growth [21]. Moreover, growth strongly depends on substrate flux and chemical activity of the compounds. By setting dX/dt (Eq. 3) to zero, the minimum chemical activity *a* (truly dissolved concentration in aqueous phase) for growth of degraders on the substrate can be calculated:

$$a_{nogrowth} = \frac{b \times K_M}{\mu_{\max} - b} \qquad (6)$$

The resulting minimum activity is 1.5·µgL^{-1} (8.5 nM) for mycobacteria on PHE, and 0.4-1.5·µg L^{-1} (2-8 nM) on PYR. The values are surprisingly similar to those found for growth of Gram-positive strains on PHE (6 to 11 nM PHE) [5]. All results are sufficiently far below water solubility and strains grow on PHE and PYR. However, the water solubility of the higher molecular PAH, such as benzo(a)pyrene, chrysene, indeno(1,2,3-cd)pyrene, and dibenz[a,h]-anthracene, is lower. If the degrader strains metabolize the higher molecular weight PAH with the same efficiency (i.e. the same kinetic data) as found for PHE and PYR, their use as sole growth substrate is then limited, as shown in previous experiments [6]. The water solubility of benzo(a)pyrene is at 4.5 µgL^{-1} (18 nM), that of dibenz[a,h]anthracene at 2.5·µgL^{-1} (9 nM), and that of indeno(1,2,3-cd)pyrene only at 0.5·µgL^{-1} (1.8 nM) [18]. This means that even if the pure substance is present in neighborhood to an aqueous phase, the solubility is almost too low to support bacterial growth on these substances. The only way for biodegradation is then co-metabolism, i.e. growth of degrader strains on another, more

soluble substrate. This is not based on the genetic or enzymatic potential of the degrading bacteria, but on dissolution kinetics and water solubility which limit the PAH flux towards the cells.

4.4. Modification of the model approach for simulation of aging in soils and sediments.

The ultimate goal of the model development was to provide a tool for simulating remediation options for PAH contaminated sites. Desorption of aged PAH from soils and sediments can be described by a bi-phase kinetics, with a fast and a slow desorption rate, as suggested by Johnson et al. [22]. We therefore replaced the dissolution term for PAH crystals (eq. 1) with a rapid ad/desorption to soil and a slow sequestration/remobilization step following in series:

$$\frac{dm_D}{dt} = -k_{DA}\ m_D\ + k_{AD} m_A - \frac{dm_M}{dt} + source \quad (7)$$

$$\frac{dm_A}{dt} = +k_{DA} m_D - k_{AD} m_A\ + k_{SA} m_S - k_{AS} m_A \quad (8)$$

$$\frac{dm_S}{dt} = +k_{AS} m_A\ - k_{SA} m_S \quad (9)$$

where D is the index for the mass of substance in the truly dissolved phase (synonymous to W water phase in eq. 1, 2 and 4), A is for adsorbed phase (rapid) and S is for sequestration (slow). The model was parameterized for PHE (K_d = 162 Lkg^{-1}), the exchange rates k were set to k_{AD} = 0.09 d^{-1} and k_{SA} = 1.73x10^{-3} d^{-1} [23], and are within the range given by Johnson et al. [22]. The backward rates are these values multiplied with K_d.

4.5. Simulations of remediation options.

The unified model [24] for mass transfer, sorption, sequestration and metabolism was also applied for the simulation of typical scenarios and remediation options.

In the first scenario, representing a typical **fresh contamination** of a soil, the source of PAH is an oil phase with 1 g PHE distributed evenly over a volume of 1 m^3. PHE dissolves within a

few days into the dissolved phase (D), from where rapid adsorption (A) and subsequent sequestration take place (Fig. 3a). A degrader population with kinetic data of *Sphingobium yanoikuyae* (Y = 0.21 $g \cdot g^{-1}$, v_{max} = 18 $g \cdot g^{-1} \cdot d^{-1}$) [5], i.e. the most efficient strain tested in previous experiments [5], grows vividly until the substrate in D and then also in A is depleted and then declines. The remaining substrate ends up in almost equal parts in A and S. Despite sufficient substrate present for further growth, it is not available for the degrader population, and the PAH in soil is "aged" and persists (Fig. 3a).

Starting from a **soil with aged contamination**, e.g. an aged contaminated site with NAPL, coal and coke material (the outcome of simulation 1) with a PHE residual mass in 1 m^3 soil of 0.08 g, 61% hereof in S, 39% in A and 0.2% in D, and initial microbial biomass X(0) = $7 \times 10^{-4} \cdot gm^{-3}$, several remediation options were simulated. **Bioaugmentation** is simulated by the **addition of degrader bacteria** (X = 0.05 gm^{-3}) after 2 years (t = 730 d) (Figure 3b). An effect is visible as a reduction of A and D (the "bioavailable" fraction), but the change is small and rarely affects the sequestered substrate in S. Within short time, the bacterial population declines again. This scenario may be the background for many failed bioremediation approaches in real contaminated sites. Unfortunately, most of these reports are only published in the `grey´ literature about remediation actions; nevertheless, some of them are also mentioned in peer-reviewed literature [25, 26].

An alternative strategy is the addition of **adsorbing amendments to soil** [27, 28], which we simulated by a ten-fold increased organic carbon content of the soil, equivalent to a **ten-fold increase of K_d** (Fig. 3c). Practically all substrate remains present adsorbed (A) or sequestered (S) and bacterial degraders X decline further. The PAH exposure and toxicity may be reduced by this measure, but the biodegradation is not stimulated. This scenario is presumably realised in many contaminated sites of former gas work sites, in which particulate waste coal and coke materials were added for solidification of waste liquid coal tars finally resulting in non-bioavailable and non-degradable residual concentrations [9].

The opposite strategy of **increasing the dissolution** (decrease of desorption rate K_d) is simulated by taking 10fold less organic carbon into account. Reduced adsorption can be achieved in practice by the addition solvents or chelators. Increased solubility stimulates bacterial degradation (Fig. 3d), substrate is removed from D and A, and subsequently also the sequestered pool declines. This scenario was realised by addition of surfactants in particular, using alcohol ethoxylates or glycoside-based surfactants that are found to improve the PAH degradation [29, 30], or by organic solvents such as acetone [31]. However, higher dissolved concentrations of PAH might result in higher toxicity.

The last scenario is **co-metabolism**, and it is simulated with a constant (and high) bacterial biomass X of 0.01 $g \cdot m^{-3}$ (Fig. 3e). In the long run, this seems the most successful bioremediation strategy, because it leads to a constant and steady decline of PAH in all pools. This scenario may explain the increase of PAH after compost addition to soil [27, 28, 32, 33].

6. Conclusions

Highly sorptive materials, e.g. black carbon (BC) materials and NAPLs like tar or mineral oils, are often found in contaminated gas work sites [9]. Tar oils are hydrophobic NAPLs like crude oil and contain various amounts of PAH. Raoult´s law was shown to determine the chemical activity and thereby the mass transfer of each compound from the NAPL to the water phase according to the molar fraction of each compound in the tar oil [3, 34-38]. After decades of being dumped in the subsurface the majority of the tar oil residues are biodegraded except of those being associated to coal and coke particles [9]. Due to the degradation of low molecular weight compounds in aged tar oil NAPLs and the enrichment of amphiphilic molecules at the NAPL water interphase, the viscosity of the interface between the remaining tar oil and the water may increase. This results in an additional decrease of the mass transfer from the NAPL to the water phase. The contamination history and the structure

and composition of the soil material thus determine the outcome of bioremediation treatments. In the real world temperature and soil water content also modify the degradation rates [12].

The simulations offer distinct prospective power for the assessment of remediation options of contaminated soils. At aged sites, degrader strains cannot grow due to limited substrate availability and thus the effect of their addition (bioaugmentation) is marginal and short-termed. Moreover, a high abundance of PAH degrader communities in practically all investigated soils - including pristine soils - has been confirmed for naphthalene and PHE [8]. It can be concluded that amendment with degrader bacteria is not stimulating PAH degradation significantly over extended time spans in most cases. The addition of sorbents like biochar may decrease the bioavailable fraction and thus lower plant uptake and toxicological risk but will increase the persistence of the residual fraction due to a very limited substrate availability. Desorption flux can be stimulated by solvents (e.g. acetone) or surfactants (in best case those that can be used as substrate by the bacteria), which, however, also increases toxicity and risk of leaching. Bacterial growth can also be stimulated with complex co-substrates (compost, root exudates) enhancing co-metabolism and the bioavailability of sorbed PAH and resulting in a long-term increase of PAH degradation rates.

Supporting Material

Additional information noted in the text is available.

Conflict of interest

The authors declare no competing financial interest.

Acknowledgement

448 This research Project was financially supported by the European Union (Project ‘‘Molecular
449 Approaches and MetaGenomic Investigations for optimizing Clean-up of PAH contaminated
450 sites, MAGICPAH, Grant Agreement No. 245226) and by the Helmholtz Centre for
451 Environmental Research UFZ. The unified model with description is available in a public
452 version at http://www.magicpah.org/links/ or http://homepage.env.dtu.dk/stt/. We also thank
453 reviewer 2 for valuable comments to improve the manuscript.

454

References

[1] H.J. Hassett, W.L. Banwart, The sorption of nonpolar organics by soils and sediments, in: B.L. Sahwney, K. Brown (Eds.) Reactions and Movement of organic chemicals in soils, SSSA Special Publication No. 22, Soil Science Society of America, American Society of Agronomy, Madison, Wisconsin, USA, 1989.

[2] P.G. Wislocki, A.Y.H. Lu, Carcinogenicity and mutagenicity of proximate and ultimate carcinogens of polycyclic aromatic hydrocarbons, in: S.K. Yang, B.D. Silverman (Eds.) Polycyclic aromatic hydrocarbon carcinogenesis: structure-activity relationships, CRC-Press, Boca Raton, 1988, pp. 1-30.

[3] M. Kästner, Degradation of aromatic and polyaromatic compounds, in: H.-J. Rehm, G. Reed, A. Pühler, P. Stadler (Eds.) Biotechnology, 2nd Edition, Vol. 11b; Environmental Processes, Wiley-VCH, Weinheim, 2000, pp. 211-239.

[4] C.E. Cerniglia, M.A. Heitkamp, Microbial metabolism of polycyclic aromatic hydrocarbons (PAH) in the aquatic environment, in: U. Varanasi (Ed.) Metabolism of polycyclic aromatic hydrocarbons in the aquatic environment, CRC Press, Boca Raton, 1989, pp. 41-68.

[5] I.K.U. Adam, A. Rein, A. Miltner, A.C. da Costa Fulgêncio, S. Trapp, M. Kästner, Experimental results and integrated modeling of bacterial growth on an insoluble hydrophobic substrate (phenanthrene), Environ. Sci. Technol., 48 (2014) 8717-8726.

[6] R.A. Kanaly, S. Harayama, Advances in the field of high-molecular-weight polycyclic aromatic hydrocarbon biodegradation by bacteria, Microb Biotechnol, 30 (2010) 136-164.

[7] A. Bjørseth, T. Ramdahl, Sources and emissions of PAH, in: A. Bjørseth, T. Ramdahl (Eds.) Handbook of polycyclic aromatic hydrocarbons, Marcel Dekker, New York, 1985, pp. 1-20.

[8] A.R. Johnsen, U. Karlson, PAH degradation capacity of soil microbial communities - Does it depend on PAH exposure?, Microb. Ecol., 50 (2005) 488-495.

481 [9] U. Wiesmann, Der Steinkohleteer und seine Destillationsprodukte - Ein Beitrag zur
482 Geschichte der Technik und der Bodenverschmutzung, in: B. Wiegert (Ed.) Biologischer
483 Abbau von polyzyklischen aromatischen Kohlenwasserstoffen, SFB 193, TU Berlin, Berlin,
484 1994, pp. 3-18.
485 [10] M. Alexander, Aging, bioavailability, and overestimation of risk from environmental
486 pollutants, Environ. Sci. Technol., 34 (2000) 4259-4265.
487 [11] K.J. Doick, E. Klingelmann, P. Burauel, K.C. Jones, K.T. Semple, Long-term fate of
488 polychlorinated biphenyls and polcyclic aromatic hydrocarbons in an agricultural soil,
489 Environ. Sci. Technol., 39 (2005) 3663-3670.
490 [12] M. Kästner, K.M. Nowak, A. Miltner, S. Trapp, A. Schäffer, Classification and modelling
491 of non-extractable residue (NER) formation of xenobiotics in soil - a synthesis, Crit. Rev.
492 Environ. Sci. Technol., 44 (2014) 2107-2171.
493 [13] L.Y. Wick, T. Colangelo, H. Harms, Kinetics of mass transfer-limited bacterial growth on
494 solid PAHs, Environ. Sci. Technol., 35 (2001) 354-361.
495 [14] C.T. Hennessee, J.S. Seo, A.M. Alvarez, Q.X. Li, Polycyclic aromatic hydrocarbon-
496 degrading species isolated from Hawaiian soils: *Mycobacterium crocinum* sp. nov.,
497 *Mycobacterium pallens* sp. nov., *Mycobacterium rutilum* sp. nov. and *Mycobacterium*
498 *aromaticivorans* sp.nov., Int. J. Syst. Evol. Microbiol., 59 (2009) 378-387.
499 [15] DSMZ, Mineral Medium (Brunner) with Vitamins, in, 2010.
500 [16] I.N. Bronstein, K.A. Semendyayev, G. Musiol, H. Muehlig, Handbook of Mathematics,
501 7th German ed., Verlag Harri Deutsch, Frankfurt/Main, 2008.
502 [17] I.K.U. Adam, A. Rein, A. Miltner, A.C. da Costa Fulgêncio, S. Trapp, M. Kästner,
503 Experimental results and integrated modeling of bacterial growth on an insoluble
504 hydrophobic substrate (phenanthrene). Environmental Science & Technology, 48 (2014)
505 8717-8726.
506 [18] G. Rippen, Handbuch Umweltchemikalien - Stoffdaten - Prüfverfahren - Vorschriften,
507 ecomed Verlagsgesellschaft, Landsberg am Lech, 1990.

508 [19] S. Trapp, A. Franco, D. Mackay, Activity-based concept for transport and partitioning of
509 ionizing organics, Environ. Sci. Technol., 44 (2010) 6123-6129, incl. Supporting Information.
510 [20] J.J. Pignatello, B.S. Xing, Mechanisms of slow sorption of organic chemicals to natural
511 particles, Environ. Sci. Technol., 30 (1996) 1-11.
512 [21] D.K. Button, Kinetics of nutrient-limited transport and microbial growth, Microbiol. Rev.,
513 49 (1985) 270-297.
514 [22] M.D. Johnson, T.M. Keinath, W.J. Weber, A distributed reactivity model for sorption by
515 sails and sediments. 14. Characterization and modeling of phenanthrene desorption rates,
516 Environ. Sci. Technol., 35 (2001) 1688-1695.
517 [23] S. Trapp, M. Kästner, I.K.U. Adam, A. Rein, U. Gosewinkel Karlson, Methods for
518 improvement of PAH degradation by substrate amendments, solvent and phytoremediation,
519 in, Project Molecular Approaches and Metagenomic Investigations for Optimizing Clean-up of
520 PAH-contaminated Sites (MagicPAH), EU FP 7 KBBE-2009-3-5-01, Deliverable 36, 2014.
521 [24] S. Trapp, A. Rein, Predictive model for PAH degradation and residue formation related
522 to bioavailability, in, Project Molecular Approaches and Metagenomic Investigations for
523 Optimizing Clean-up of PAH-contaminated Sites (MagicPAH), EU FP 7 KBBE-2009-3-5-01,
524 Magic PAH Deliverable 23, available at
525 http://homepage.env.dtu.dk/stt/Magic%20PAH/Magic%20PAH%20Deliverable%2023.pdf,
526 last retrieved 13 May 2015, 2012.
527 [25] C. García-Delgado, A. D'Annibale, L. Pesciaroli, F. Yunta, S. Crognale, M. Petruccioli, E.
528 Eymar, Implications of polluted soil biostimulation and bioaugmentation with spent mushroom
529 substrate (*Agaricus bisporus*) on themicrobial community and polycyclic aromatic
530 hydrocarbons biodegradation., Science of the Total Environment 508 (2015) 20-28.
531 [26] N. Loick, P.J. Hobbs, M.C.D. Hale, D.L. Jones, Bioremediation of Poly-Aromatic
532 Hyrdocarbon (PAH)-Contaminated Soil by Composting., Crit. Rev. Environ. Sci. Technol., 39
533 (2012) 271-332.

534 [27] G. Marchal, K.E.C. Smith, A. Rein, A. Winding, L.W. de Jonge, S. Trapp, U.G. Karlson,
535 Impact of activated carbon, biochar and compost on the desorption and mineralization of
536 phenenthrene in soil, Environ. Pollut., 181 (2013) 200-210.
537 [28] G. Marchal, K.E.C. Smith, A. Rein, A. Winding, S. Trapp, U.G. Karlson, Comparing the
538 desorption and biodegradation of low concentrations of phenanthrene sorbed to activated
539 carbon, biochar and compost, Chemosphere, 90 (2013) 1767–1778.
540 [29] T. Madsen, P. Kristensen, Effects of bacterial inoculation and nonionic surfactants on
541 degradation of polycyclic aromatic hydrocarbons in soil., Environmental Toxicology and
542 Chemistry, 16 (1997) 631-637.
543 [30] M. Megharaj, B. Ramakrishnan, K. Venkateswarlu, N. Sethunathan, R. Naidu,
544 Bioremediation approaches for organic pollutants: A critical perspective., Environmental
545 International, 37 (2011) 1362-1375.
546 [31] T. Grotenhuis, J. Field, R. Wasseveld, W. Rulkens, Biodegradation of polyaromatic
547 hydrocarbons (PAH) in polluted soil by the white-rot fungus *Bjerkandera*., Journal of
548 Chemical Technology and Biotechnology, 71 (1999) 359-360.
549 [32] I.K.U. Adam, A. Miltner, M. Kästner, Degradation of ^{13}C-labelled pyrene degradation in
550 soil-compost mixtures and fertilized soil, Appl. Microbiol. Biotechnol., (2015) in press.
551 [33] M. Kästner, B. Mahro, Microbial degradation of polycyclic aromatic hydrocarbons in soils
552 affected by the organic matrix of compost, Appl. Microbiol. Biotechnol., 44 (1996) 668–675.
553 [34] C. Eberhardt, P. Grathwohl, Time scales of organic contaminant dissolution from
554 complex source zones: coal tar vs. blobs, J. Contam. Hydrol., 59 (2002) 45-66.
555 [35] S. Ghoshal, A. Ramaswami, R.G. Luthy, Biodegradation of naphthalene from coal tar
556 and heptamethylnonane in mixed batch systems, Environ. Sci. Technol., 30 (1996) 1282-
557 1291.
558 [36] L.S. Lee, M. Hagwall, J.J. Delfino, P.S.C. Rao, Partitioning of polycyclic aromatic
559 hydrocarbons from Diesel fuel into water, Environ. Sci. Technol., 26 (1992) 2104-2110.
560 [37] L.S. Lee, P.S.C. Rao, I. Okuda, Equilibirum partitioning of polycyclic aromatic
561 hydrocarbons from coal tar into water, Environ. Sci. Technol., 26 (1992) 2110-2115.

562 [38] M. Wehrer, T. Rennert, K.-U. Totsche, Kinetic control of contaminant release from
563 NAPLs - Experimental evidence, Environ. Pollut., 179 (2013) 315-325.
564 [39] Metcalf, Eddy, Wastewater Engineering, Treatment and Reuse, Mc-Graw Hill, New York,
565 2003.

566

567

Figure captions

Figure 1. Experiments with *Mycobacterium rutilum*: PHE concentration in suspension C_{Sus} (—♦—) and estimated microbial protein concentration $C_{X,est}$ (-··○··-), measured (data points) versus modeled (curves). Experiments with nominal initial phenanthrene concentrations: a) C_0 = 10 mgL^{-1}, b) C_0 = 25 mgL^{-1}, c) C_0 = 50 mgL^{-1}, d) C_0 = 100 mgL^{-1}, e) C_0 = 200 mgL^{-1}, f) C_0 = 400 mgL^{-1}. Error bars indicate minimum and maximum (3 replicates).

Figure 2. Experiments with *Mycobacterium rutilum*: PYR concentration in suspension C_{Sus} (—♦—) and estimated microbial protein concentration $C_{X,est}$ (-··○··-), measured (data points) versus modeled (curves). Experiments with nominal initial pyrene concentrations: a) C_0 = 10 mgL^{-1}, b) C_0 = 25 mgL^{-1}, c) C_0 = 50 mgL^{-1}, d) C_0 = 100 mgL^{-1}, e) C_0 = 200 mgL^{-1}, f) C_0 = 400 mgL^{-1}. Error bars indicate minimum and maximum (3 replicates).

Figure 3. Simulation of remediation scenarios with the most efficient degrader strain *Sphingobium yanoikuyae*. Dissolved PHE phase (—), adsorbed PHE phase (-··), sequestered PHE phase (- -), microbial protein (•••). a) Scenario after release of 1 g PHE into 1 m^3 soil. This panel additionally shows PHE in the NAPL phase for the first 2.6. days (…). b) Bioaugmentation with microbial degrader biomass to X = 0.05 g/m^3 after 2 more years, c) Amendment with organic carbon (OC = 20%, K_d increased by a factor of 10), d) solubilisation (K_d decreased by a factor of 10), e) simulation of co-metabolism with constant X = 0.01 g·m^{-3}.

595 **Table 1.** PHE and PYR degrading strains used in the present experiments

Species	***Mycobacterium rutilum***	***Mycobacterium pallens***
DSM-No.	45405	45404
Gram staining	positive	positive
Morphology	rod-shaped	rod-shaped
Motility	-	-
Isolated from	soil from urban park in Honolulu, Hawaii, USA [14]	non-contaminated soil from Wahiawa, Hawaii, USA [14]
PAH mineralization	PHE, PYR	PHE, FLU, PYR

596 (PHE: phenanthrene, FLU: fluoranthene, PYR: pyrene)

597

598

599 **Table 2.** Model parameters and related fitted Monod parameters for the *Mycobacterium*
600 strains

Parameters	Symbol	Value	Unit	Reference / comment
Input parameters				
Suspension volume	V_{Sus}	0.1	L	
PHE density	ρ_{ph}	1100	kg m^{-3}	[18]
PYR density	ρ_{ph}	1270	kg m^{-3}	[18]
PHE water solubility	S	1.15	g m^{-3}	[18]
PYR water solubility	S	0.135	g m^{-3}	[18]
Microbial protein fract.	$f_{m,prot}$	0.55	g prot g^{-1} biomass	[39]
Fitted parameters – Dissolution flux				
PHE permeability x f_A	$P \times f_A$	160 (120-200)	m d^{-1}	details see SM
PYR permeability x f_A	$P \times f_A$	475 (400-550)	m d^{-1}	details see SM
Fitted parameters – Monod				
Mycobacterium rutilum and PHE degradation				
Half-saturation const.	K_M	0.1	g m^{-3}	
Yield	Y	0.20 (0.16-0.28)	g bact g^{-1}	
Death rate const.	b	0.03	d^{-1}	
Max. removal rate	v_{max}	10 (7-12)	g g^{-1} bact d^{-1}	
Mycobacterium rutilum and PYR degradation				
Half-saturation const.	K_M	0.1	g m^{-3}	
Yield	Y	0.22 (0.17-0.28)	g bact g^{-1}	
Death rate const.	b	0.03	d^{-1}	
Max. removal rate	v_{max}	9 (7-11)	g g^{-1} bact d^{-1}	
Mycobacterium pallens and PYR degradation				
Half-saturation const.	K_M	0.1	g m^{-3}	
Yield	Y	0.32 (0.25-0.36)	g bact g^{-1}	
Death rate const.	b	0.01	d^{-1}	
Max. removal rate	v_{max}	8 (6-10)	g g^{-1} bact d^{-1}	

601 (fitted parameters: best estimate values, with ranges in brackets; fract.: fraction; const.: constant;
602 max.: maximal; corr.: correction, bact: bacteria; prot: protein; f_A: correction factor for deviations of
603 surface area from cubic geometry)

604

Figures

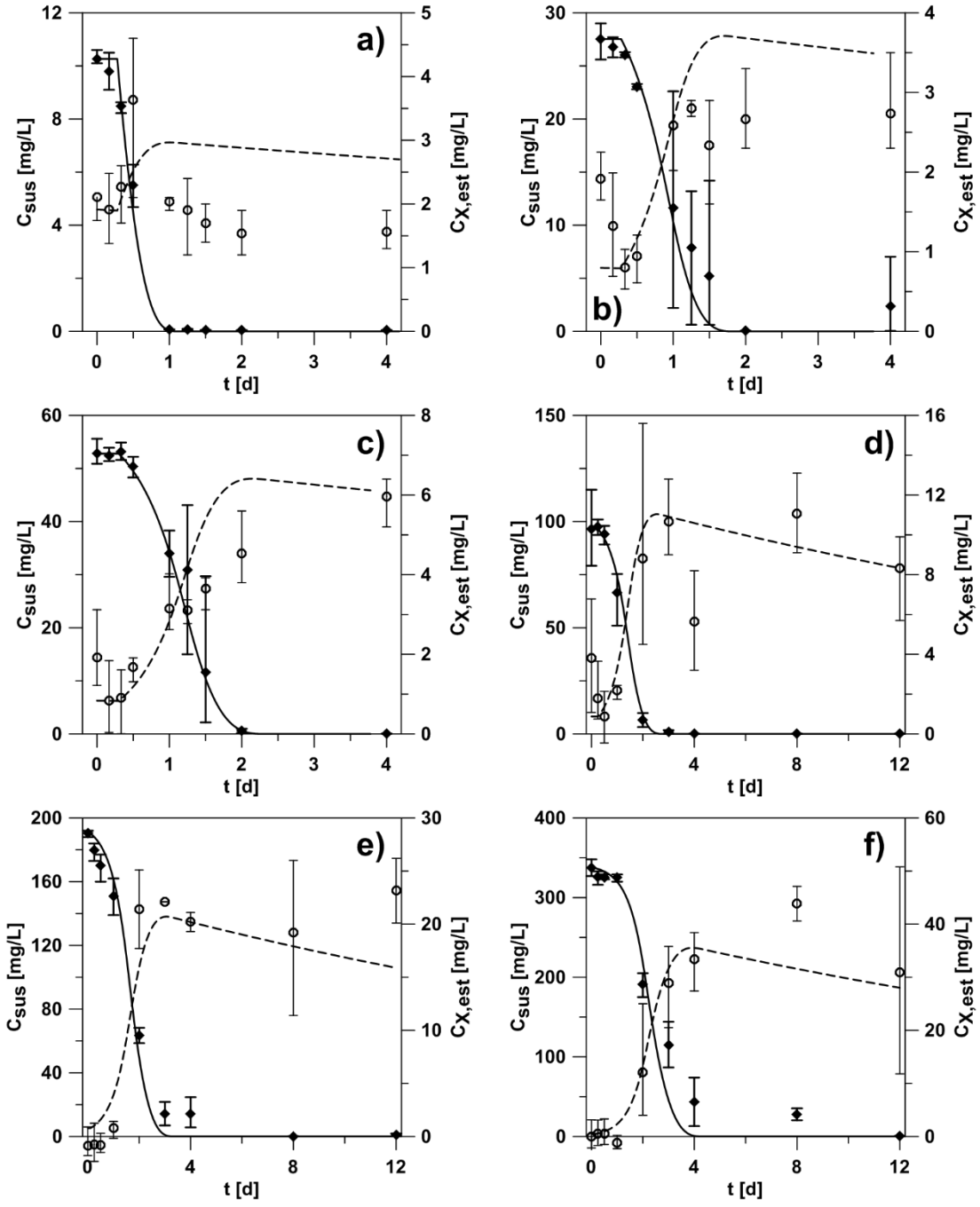

Figure 1

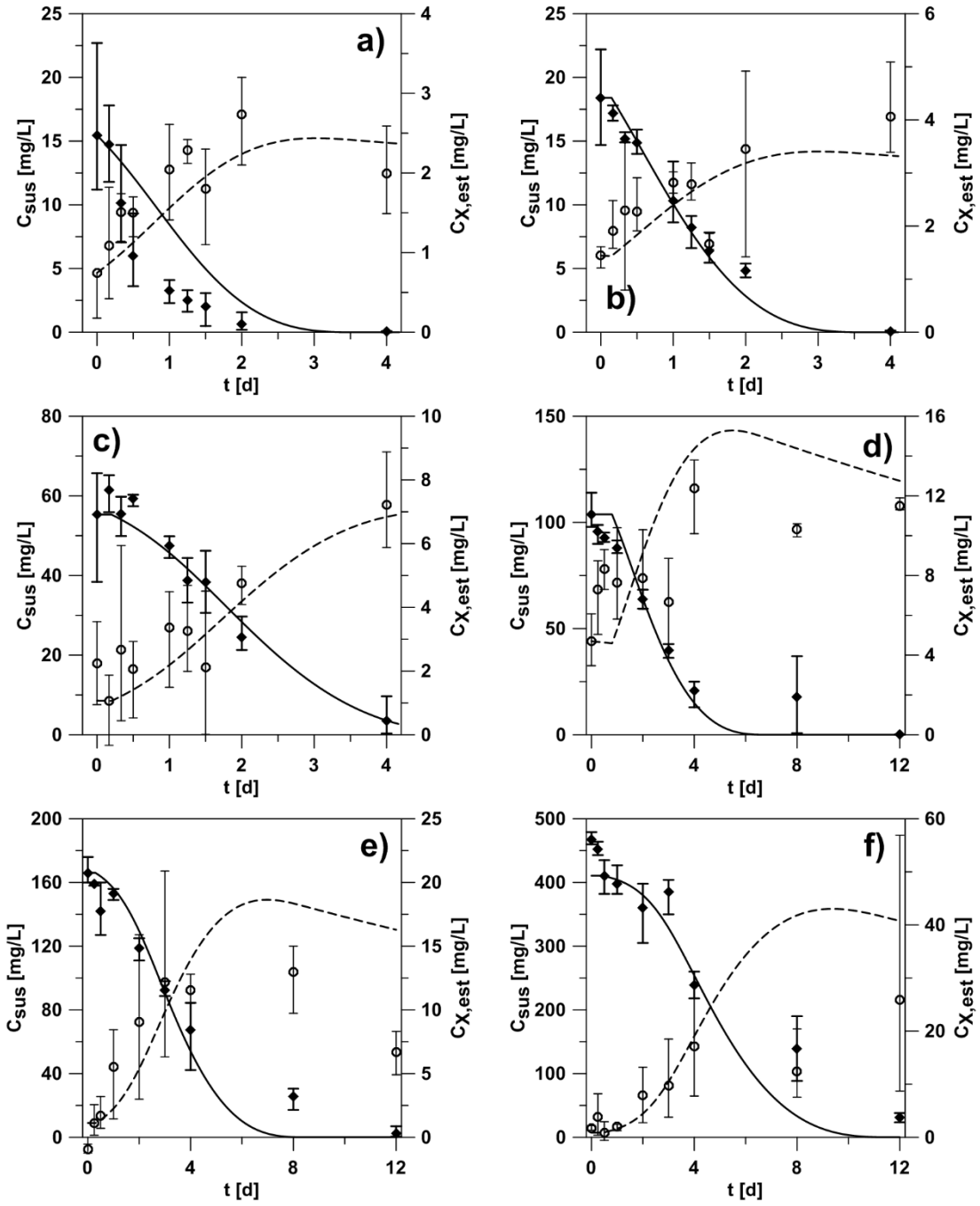

Figure 2

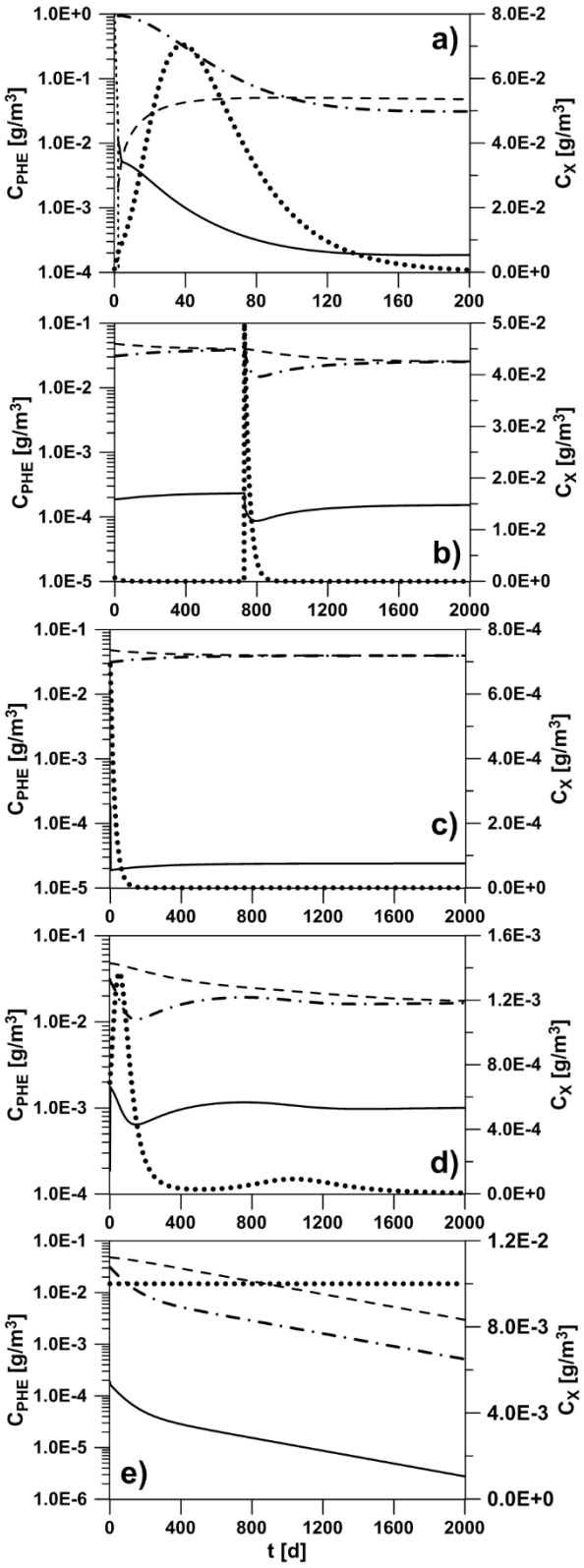

Figure 3